Biomaterials Science

ROYAL SOCIETY OF CHEMISTRY

PAPER

View Article Online
View Journal | View Issue

Published on 21 February 2025. Downloaded by Soochow University China on 4/17/2026 7:33:40 AM.

Check for updates

Cite this: *Biomater. Sci.*, 2025, **13**, 2036

Polymersome-mediated Cbl-b silencing activates T cells against solid tumors

Guanhong Cui,†[a] Yu Shao,†[b] Junyao Wang,[b] Congcong Xu, *[a,c] Jinping Zhang*[b] and Zhiyuan Zhong *[a,c,d]

Received 3rd January 2025,
Accepted 20th February 2025

DOI: 10.1039/d5bm00001g

rsc.li/biomaterials-science

Unleashing T cell function is critical for efficacious cancer immunotherapy. Here, we present an *in vivo* T cell activation strategy by silencing Casitas B-lineage lymphoma proto-oncogene b (Cbl-b), an intracellular checkpoint, to effectively combat solid tumors. The polymersomes are able to efficiently load and deliver siRNA against *cblb* to T cells both *in vitro* and *in vivo*, successfully silencing the *cblb* gene expression in primary T cells and enhancing the IL-2 receptor CD25 expression, which in turn enhances T cell function and prevents T cell exhaustion. *In vitro* and *in vivo* studies showed that siRNA against *cblb* caused an effective inhibition of tumor progression in subcutaneous B16-F10 and LLC models, in which a significant increase of effector T cells in peripheral blood mononuclear cells and an increase of effector T cells and a significant decrease of Treg cells in the tumor were clearly observed. This polymersome-mediated down-regulation of the *cblb* gene in T cells provides a promising approach for activating T cells and enhancing their anti-tumor capacity.

1. Introduction

T cells play a critical role in different cancer immunotherapy paradigms including immune checkpoint blockade (ICB) therapy, chimeric antigen receptor (CAR) T cell therapy and cancer vaccines.[1–3] The number and function of T cells largely determine the anti-tumor effect and affect the prognosis.[4,5] Enhancing the activity of T cells and preventing their exhaustion can effectively improve the anti-tumor potency,[6] as evidenced by ICB therapy which blocks the receptors and ligands involved in pathways that attenuate T cell activation such as programmed death 1 (PD-1) and cytotoxic T lymphocyte-associated antigen 4 (CTLA-4).[7] However, ICB therapy works only on a minority of patients,[8,9] partly due to the presence of intracellular pathways that negatively regulate T cell activation.[10,11]

E3 ubiquitin ligase Cbl-b has been identified as an intracellular immune inhibitor protein and a goalkeeper to prevent the undesired activation of T cells, which is critical for the expansion of T cells to maintain the balance between anergy and activation.[12,13] Cbl-b controls the threshold of T cell activation, and *cblb*-deficiency in naive T cells unlocks the requirement of CD28 co-stimulation from the activation of T cells for effective proliferation and interleukin-2 (IL-2) secretion.[14] Currently, different therapeutic modalities targeting Cbl-b have been investigated in clinical trials including small molecule inhibitors (NX-1607, NCT05107674),[15,16] *cblb* gene edited autologous CAR-T (bbT369, NCT05169489), and *cblb* siRNA electroporated PBMCs (APN401, NCT06172894).[17,18] Accumulated evidence suggests that *in vitro* silencing of *cblb* in T cells inhibits cellular depletion and enhances the antitumor effect of adoptive cell transfer (ACT) therapy.[19–21] However, ACT suffers from laborious *in vitro* cell expansion and/or genetic engineering procedures to generate a potent tumor-reactive $CD8^+$ T cell phenotype.[22]

Here, we report an *in vivo* T cell activation strategy by polymersome-mediated delivery of *cblb* siRNA (PsiCbl-b) to T cells for cancer immunotherapy (Scheme 1). The transfection of T cells *in vivo* is challenging.[23–25] We previously developed a chimeric polymersome platform that can efficiently deliver siRNA therapeutics to different tumor models such as ovarian, pancreatic, and brain metastatic breast cancer.[26–28] It is intriguing that PsiCbl-b achieves significant downregulation of the *cblb* gene in T cells both *in vitro* and *in vivo*, which also upregulates CD25 (the receptor of IL-2) and improves the anti-tumor immunity of T cells. Further therapeutic results in B16-F10 melanoma and LLC tumor models reveal effective tumor inhibition.

[a]*Biomedical Polymers Laboratory, College of Chemistry, Chemical Engineering and Materials Science, and State Key Laboratory of Radiation Medicine and Protection, Soochow University, Suzhou, 215123, P. R. China. E-mail: xucc@suda.edu.cn, zyzhong@suda.edu.cn*

[b]*Institutes of Biology and Medical Sciences, Soochow University, Suzhou, 215123, P.R. China. E-mail: j_pzhang@suda.edu.cn*

[c]*International College of Pharmaceutical Innovation, Soochow University, Suzhou, 215222, P.R. China*

[d]*College of Pharmaceutical Sciences, Soochow University, Suzhou, 215123, P. R. China*

†These authors contributed equally to this work.

This journal is © The Royal Society of Chemistry 2025

Published on 21 February 2025. Downloaded by Soochow University China on 4/17/2026 7:33:40 AM.

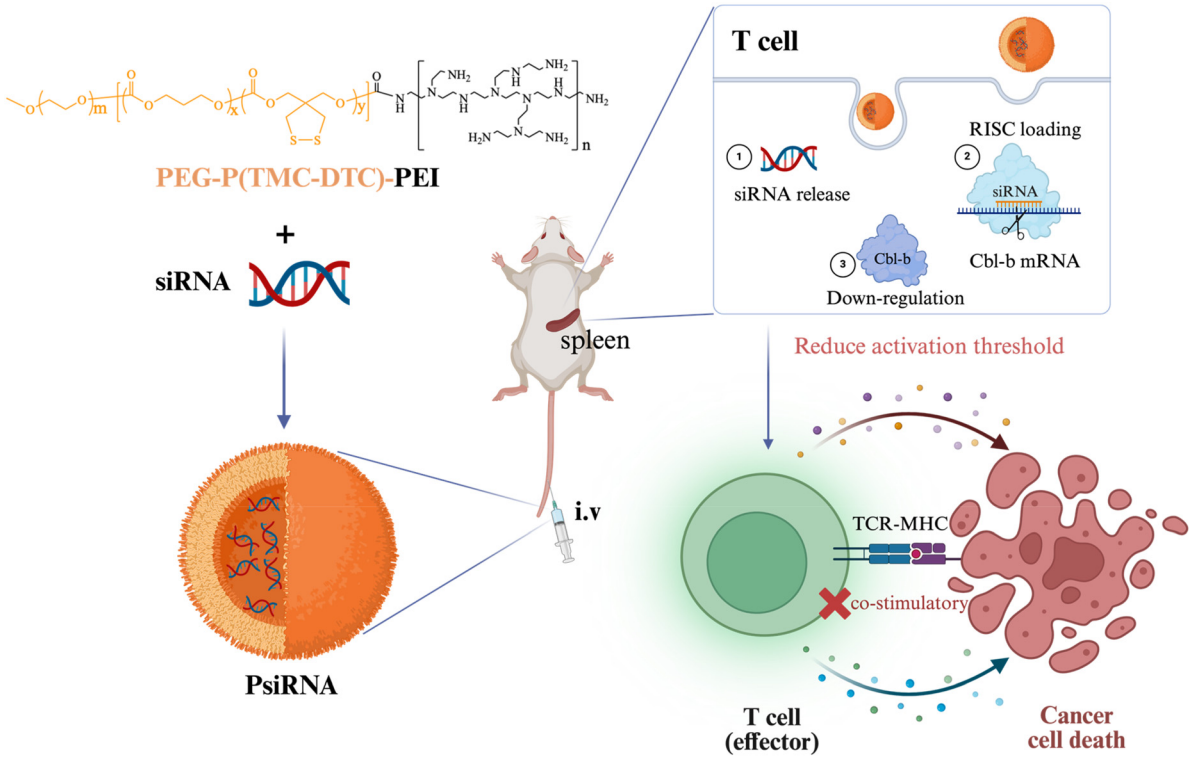

Scheme 1 Schematic illustration of the construction of PsiRNA for Cbl-b down-regulation in T cells which leads to reduced activation threshold and enhanced anti-tumor efficacy.

2. Results and discussion

Design and fabrication of PsiCbl-b

Based on the coding sequence of *cblb* mRNA, three target regions were selected for siRNA design as following: Cbl-b-1 CCCACCGTATATACTTGAT, Cbl-b-2 GCAATATCCTACAGACCAT and Cbl-b-3 GCTCCGAGCAGGTTCTTAT. To analyze the silencing efficacy, we used Lipofectamine™ 2000 to co-transfect the Cbl-b over-expression plasmid and siRNA (siCbl-b-1, siCbl-b-2, and siCbl-b-3, respectively) in HEK293T cell line. Quantitative real-time PCR (qPCR) and western blot results suggested that siCbl-b-3 led to 69% *cblb* mRNA silencing and nearly complete protein knock-down (Fig. 1A and B). Therefore, siCbl-b-3 was employed as the experimental siRNA sequence in subsequent experiments.

To deliver siRNA molecules *in vivo* for T cell modulation, the polymersome-based nanoparticle (NP) delivery system was exploited as previously reported.[26,27] In brief, NPs were readily fabricated by adding a solution of poly(ethylene glycol)-*b*-poly (trimethylene carbonate-*co*-dithiolane trimethylene carbonate)-polyethyleneimine (abbreviated as PEG-P(TMC-DTC)-PEI) into phosphate buffer containing siRNA followed by dialysis. After the formation of NPs, the relatively long hydrophilic PEG chain and hydrophobic ester segments allowed PEG to be presented on the outer surface, while positively- charged PEI located in the core. The repeating units of DTC enabled reversible crosslinking of polymers and responsive breaking down of disulfide bonds under reducing conditions such as in the cytosol. NPs with hydrophilic cavities can load siRNAs through hydrophilic–hydrophobic interactions and adsorb siRNAs inside NPs more efficiently by electrostatic interactions with positively-charged PEI tertiary amino groups.[29,30] When the designed polymer was mixed with siRNA at 10 wt% of polymer, the formed PsiRNA showed a size of ~50 nm as characterized by dynamic light scattering (DLS) and transmission electron microscopy (TEM) imaging (Fig. 1C). Agarose gel electrophoresis of PsiRNA complexes with various siRNA weight ratios indicated that siRNA loading efficiency was nearly 100% with 10% siRNA weight ratio (Fig. 1D). When the siRNA reached 15 wt% of the polymer or above, siRNA could not be stably loaded in vesicles, indicating that the loading capacity of NPs was close to saturation at 10% siRNA weight ratio. Thus a 10% siRNA weight ratio was chosen for subsequent polymersome preparation. We next verified the transfection efficiency of the PsiCbl-b complex on HEK293T cells. With an increasing dosage of PsiCbl-b-3, the target *cblb* mRNA and flag-tagged Cbl-b protein showed more significant down-regulation (Fig. 1E and F). To assess the cytotoxicity of PsiCbl-b to primary T cells, we performed the CCK-8 assay by treating primary T cell with a serial concentration of NPs. Even at 200 μg NPs equiv. per mL, an 8-fold higher dosage than that used for *in vitro* experiments, negligible toxicity was observed. Instead, a higher cell viability was observed (Fig. 1G) which might be explained by the benefit of Cbl-b silencing.[12,13]

Published on 21 February 2025. Downloaded by Soochow University China on 4/17/2026 7:33:40 AM.

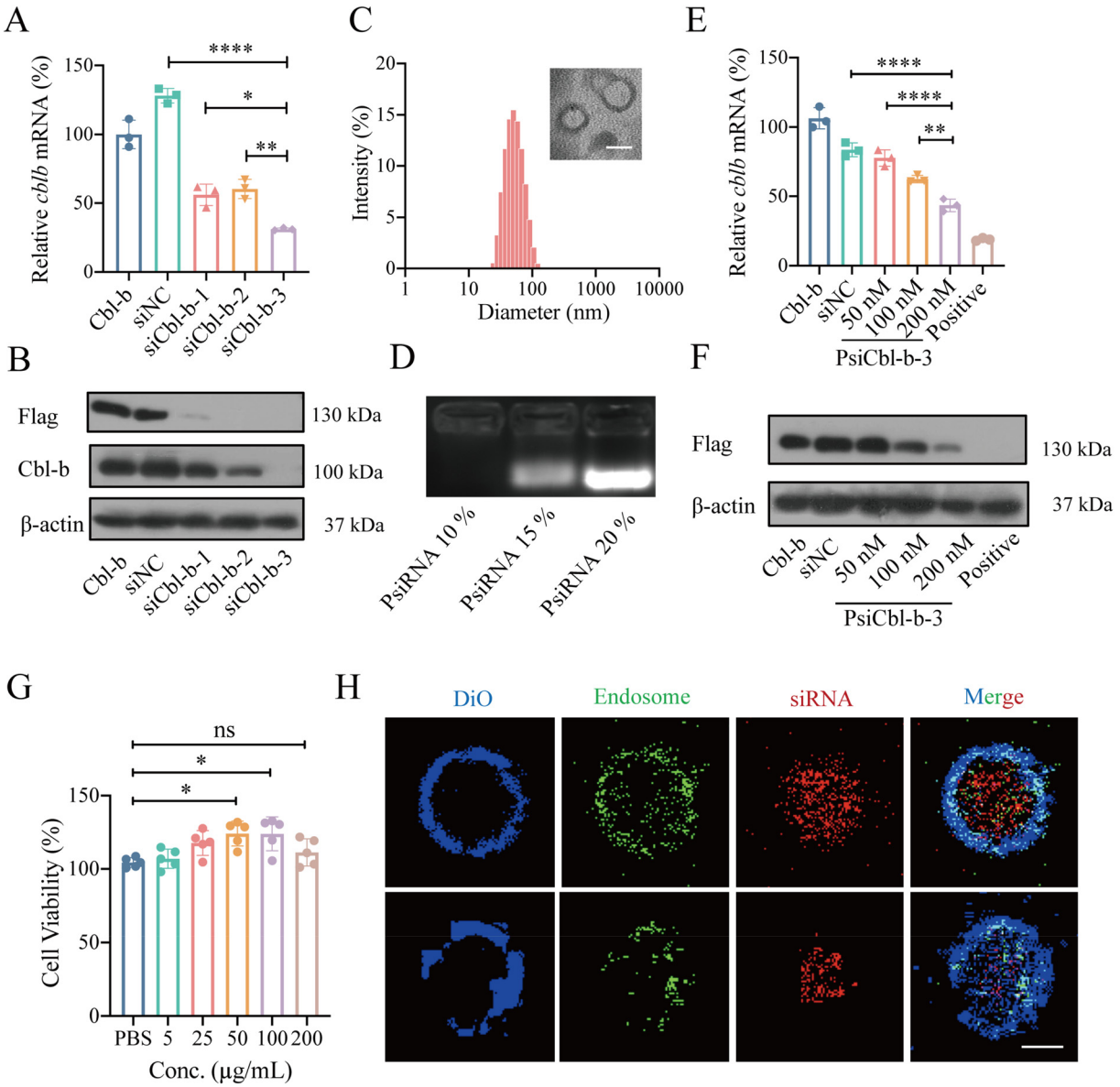

Fig. 1 *In vitro* formulation, characterization, and cellular uptake of PsiRNA. (A) Co-transfection of the Cbl-b over-expression plasmid and siRNA with Lipofectamine™ 2000 in HEK293T cell line for siRNA screening by qPCR (n = 3). (B) Western blot analysis showing the down-regulation of Cbl-b with siCbl-b sequences. (C) Size distribution of PsiRNA determined by DLS and TEM, scale bar: 50 nm. (D) Agarose gel electrophoresis characterization of the siRNA loading efficiency. (E and F) Dosage-dependent silencing of *cblb* in HEK293T cells after the transfection of PsiCbl-b. (E) The *cblb* silencing efficiency was determined by qPCR (n = 3), and (F) the Flag-Cbl-b protein expression was observed by the Western blot assay. Positive lane indicates transfection of siRNA using Lipofectamine™ 2000. (G) Cell viability of primary T cells at 24 h post-incubation with varying concentrations of PsiCbl-b (n = 5). (H) Confocal microscopy imaging showing the endosomal escape of PsiRNA^{Cy5} in primary T cells at 4 h post-incubation. Scale bar, 5 μm. P value: *p < 0.05; **p < 0.01; ****p < 0.0001.

PsiRNA facilitated the cell entry *via* endocytic pathway, whereas the endosomal release of siRNA is critical for forming functional RNA-induced silencing complex (RISC) with Argonaute protein in cytosol.[31,32] We conducted confocal microscopy imaging to evaluate the endosome escape of PsiRNA at 4 h. Results indicated that most of the Cy5-labeled siRNA molecules escaped to the cytoplasm with little colocalization with endosomes (Fig. 1H). Pearson's colocalization coefficient was calculated as 0.22 ± 0.16, suggesting a weak colocalization correlation between siRNA molecules and endosomes. The efficient endosome escape of siRNA in primary T cells would contribute to an efficient gene silencing effect.

In vitro primary T cells activation by PsiCbl-b

To evaluate the *cblb* silencing effect of PsiCbl-b on primary T cells, the collected T cells from C57BL/6 mice were incubated with PsiCbl-b followed by quantification of *cblb* mRNA and Cbl-b protein. A remarkable down-regulation of the *cblb* level

 This journal is © The Royal Society of Chemistry 2025

Published on 21 February 2025. Downloaded by Soochow University China on 4/17/2026 7:33:40 AM.

was observed (Fig. 2A and B). Next, we evaluated the immunostimulatory effects of PsiCbl-b on primary T cells. The secreted IFN-γ and TNF-α were observed with a 1.7 and 1.5-fold increase respectively in the supernatant of the PsiCbl-b treated T cell medium compared to the PsiNC group (Fig. 2C). Moreover, the frequency of $CD3^+CD25^+$ T cells treated with PsiCbl-b was upregulated 1.3-fold compared with that of the PBS group, indicating an obvious naive T cell activation (Fig. 2D and E) in the absence of co-stimulatory receptor signaling.[14]

To assess whether the improved T cell functionality will lead to enhanced anti-tumor effects *in vivo*, we then infused the PsiCbl-b transfected T cells back into mice. T cells were sorted from healthy mice spleen and treated with PBS (untreated group), empty vehicle NPs, PsiNC and PsiCbl-b respectively. After co-incubation for 3 days, 2×10^6 pre-treated T cells were intravenously injected into the mice. On the same day, 2×10^5 EL4 cells were inoculated subcutaneously on the right flank of mice and tumor growth was monitored (Fig. 2F). We were excited to note that T cells transfected with PsiCbl-b produced significant anti-tumor effects in the mice within 9 days post-administration compared to PsiNC and empty vehicle groups (Fig. 2G). These results demonstrated that Cbl-b down-regulation boosted T cell anti-tumor activity both *in vitro* and *in vivo*, which corroborated its clinical potentials in adoptive cell therapy.[18,19]

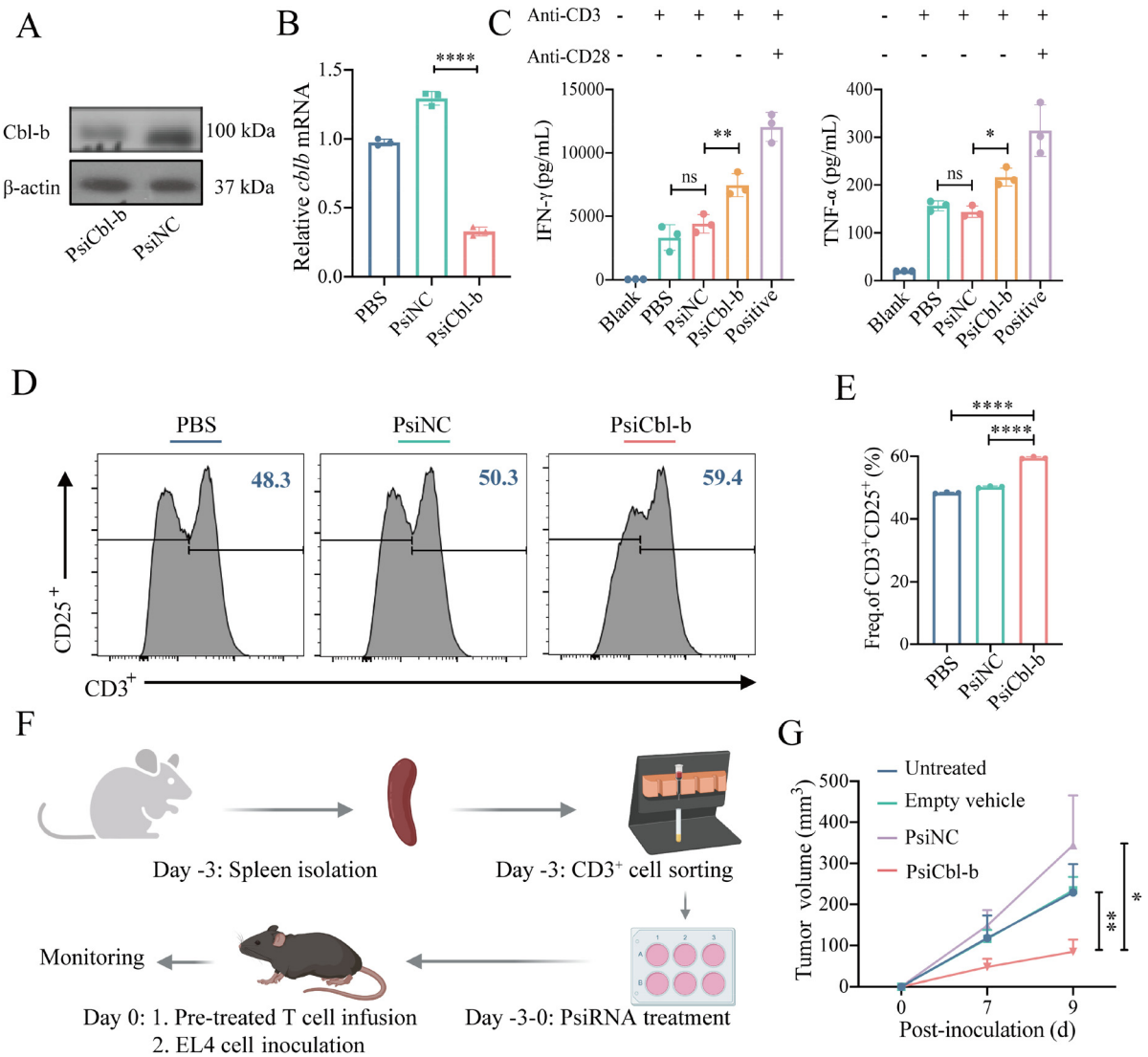

Fig. 2 *In vitro* T cell modulation by PsiCbl-b for effective tumor inhibition. (A) Down-regulation of *cblb* in primary T cells analyzed by Western blot and (B) qPCR (n = 3). (C) The secreted IFN-γ and TNF-α of primary T cells in the supernatant were detected using the ELISA assay (n = 3). (D) Expression of CD25 in T cells after treatment with PBS, PsiNC (siNC Conc. 200 nM) and PsiCbl-b (siCbl-b Conc. 200 nM) for 3 days using the FACS assay and (E) quantification of the $CD3^+CD25^+$ cell population frequency (n = 3). (F) Scheme of the animal study using *in vitro* treated T cells. T cells were isolated from the healthy spleen of C57BL/6 mice and treated with PBS (Untreated), empty vehicle, PsiNC (200 nM) and PsiCbl-b (200 nM), respectively. After 3 days, 2×10^6 T cells were infused intravenously into mice, which were inoculated with 2×10^5 EL4 cells subcutaneously on the right flank. (G) Tumor growth curve (n = 5) over the course of 9 days. P value: *$p < 0.05$; **$p < 0.01$; ****$p < 0.0001$.

Published on 21 February 2025. Downloaded by Soochow University China on 4/17/2026 7:33:40 AM.

In vivo T cell transfection by PsiCbl-b

Despite the demonstrated efficacy of *in vitro* transfected T cells in tumor inhibition, this adoptive cell transfer strategy poses challenges in clinical translation as a result of labor-intensive and long production cycle.[33] Direct T cell modulation *in vivo* holds great promise for cancer immunotherapy. Therefore, we sought to deliver siCbl-b to T cells *in vivo via* polymersomes for T cell modulation. We first evaluated the biodistribution profile of PsiRNA following intravenous injection in mice. Cy5-labeled siRNA, in its free or encapsulated form, showed a distinct *in vivo* organ distribution. The majority of free siRNA was observed in the kidneys, suggesting a fast renal clearance of siRNA owing to its small size below the glomerular filtration cut-off size. In contrast, PsiRNA elicited a 2.1-fold increase in the fluorescent intensity in spleen where major mature T cells are located (Fig. 3A and B). The spleen fluorescent intensity was 5.1-fold higher than that in the kidneys, suggesting an

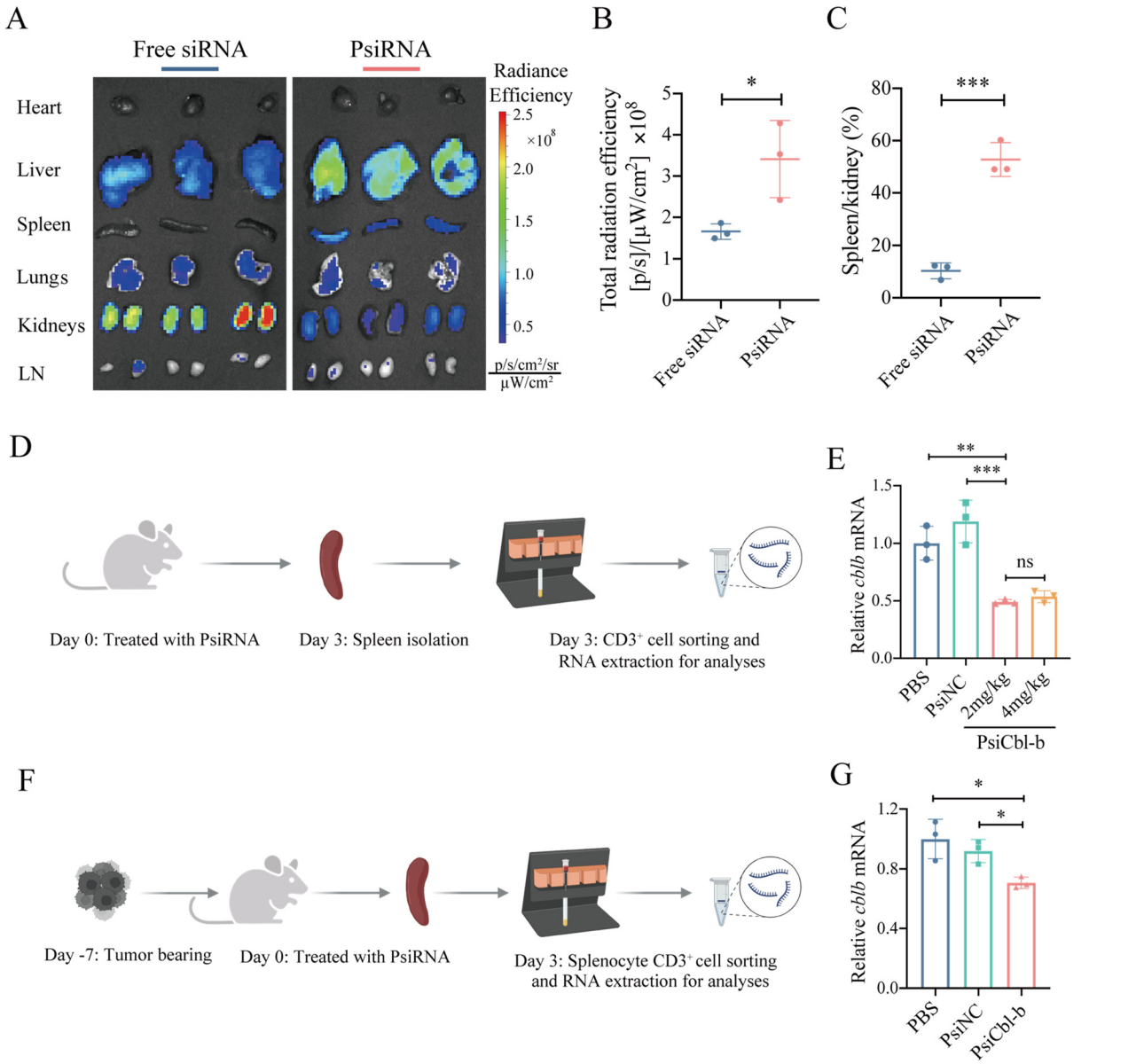

Fig. 3 Biodistribution of PsiRNA and *in vivo* silencing *cblb* gene. (A) IVIS image of the accumulation of Cy5-labeled siRNA ($siRNA^{Cy5}$) in organs after the intravenous injection of free $siRNA^{Cy5}$ and $PsiRNA^{Cy5}$ (1 mg $siRNA^{Cy5}$ equiv. per kg). (B) Quantification of total radiance efficiency in spleen (n = 3). (C) Spleen/Kidney ratio of total radiance. (D) Animal study timeline to analyze the T cell transfection efficiency *in vivo*. Healthy mice were administered with PsiRNA (2 mg or 4 mg siRNA equiv. per kg) intravenously, spleen was isolated after 3 days and $CD3^+$ cells in splenocytes were sorted for RNA extraction and qPCR assay. (E) Quantification of *cblb* gene expression in healthy mice (n = 3). (F) Animal study timeline to analyze the T cell transfection efficiency in tumor-bearing mice (2 mg siRNA equiv. per kg), and (G) quantification of *cblb* gene expression in tumor-bearing mice (n = 3). P value: *p < 0.05; **p < 0.01; ***p < 0.001.

This journal is © The Royal Society of Chemistry 2025

Published on 21 February 2025. Downloaded by Soochow University China on 4/17/2026 7:33:40 AM.

enhanced retention of siRNA in the spleen delivered by polymersomes (Fig. 3C). This will facilitate the siRNA transfection to T cells *in vivo*. Therefore, we next evaluated the *in vivo* T cell activation in healthy mice by injecting PsiRNA preparation intravenously. At 3 days after treatment, mouse $CD3^+$ T cells sorted from splenocytes were subjected to qPCR assay (Fig. 3D). We observed a near 50% *cblb* gene silencing effect by PsiCbl-b while the PsiNC control group had a negligible effect compared to the PBS group. Interestingly, a similar gene down-regulation effect was observed with both 2 mg kg^{-1} and 4 mg kg^{-1} groups (Fig. 3E). Therefore, we used 2 mg kg^{-1} dosage thereafter in subsequent animal studies.

The lack of co-stimulatory signals of tumor cells lead to immune tolerance thereby inducing tumor immune escape.[34] The expression of Cbl-b will be upregulated in the state of T cell receptor stimulation without co-stimulation.[35,36] To assess whether PsiCbl-b could induce Cbl-b silencing of T cells in tumor-bearing mice, we first inoculated tumor cells on day −7 in mice followed by I.V. administration of PsiRNA on day 0, the primary T cells were sorted on day 3 for extracting RNA and analyzing the relative *cblb* mRNA (Fig. 3F). qPCR results suggested a 29% *cblb* gene silencing effect in T cells from tumor-bearing mice (Fig. 3G).

PsiCbl-b systemically activates T cells against solid tumors *in vivo*

Next, we evaluated the treatment outcome of PsiCbl-b in the subcutaneous B16-F10 melanoma model. Mice were treated every three days from day −3 for a total of five doses with PBS, PsiNC and PsiCbl-b respectively (siRNA, 2 mg kg^{-1}, I.V.). PBMC was collected on day 12 for the FACS assay and mice were sacrificed to obtain the PBMC and tumor tissues on day 30 for the FACS assay (Fig. 4A). Over the course of study, PsiCbl-b resulted in significant tumor growth suppression compared to PBS and the PsiNC treated group (Fig. 4B).

Subsequently, we evaluated the activated T cells in PBMC three days post the last treatment. Compared to PBS-treated mice, the percentage of central memory T cells (TCM, $CD44^+CD62L^+$) and effector memory T cells (TEM, $CD44^+CD62L^-$) of PsiCbl-b treated cells were enhanced by 3.4-fold and 1.9-fold compared to that of the PBS group, respectively (Fig. 4C and D). At the end stage of tumor progression, the percentage of TCM and TEM in PBMC of mice treated with PsiCbl-b revealed a significant increase compared with PBS and PsiNC groups (Fig. 4E–G). Moreover, the results revealed that the percentage of PsiCbl-b group's TEM in tumor tissue was increased by ~1.6-fold compared to those of PBS and PsiNC groups (Fig. 4H and I). Furthermore, negative regulatory mechanisms of Treg cells are thought to be a major cause of disabling effector T cells in tumor tissues. Treg cells were decreased by ~60% after PsiCbl-b treatment compared to PsiNC (Fig. 4J). These findings indicated that PsiCbl-b mediated *cblb* silencing *in vivo* improved the activation of T cells, while, modulating the tumor immunosuppression microenvironment for enhanced anti-tumor efficacy of T cells.

To evaluate the applicability of this *in vivo* T cell activation strategy for treatment of other tumor models, we then evaluated the anti-tumor efficacy of PsiCbl-b in subcutaneous LLC tumor model. The mice were treated every three days from day −3 for a total of five doses with PBS, PsiNC and PsiCbl-b respectively (siRNA, 2 mg kg^{-1}, I.V.) as shown in Fig. 4K. The results indicated that the down-regulation of *cblb* mediated T cell activation could also significantly suppress tumor growth (Fig. 4L).

The *in vivo* T cell modulation strategy presented here requires repeated dosing of PsiRNA. To assess the safety of PsiRNA, healthy mice were treated with a dosage of 5 mg kg^{-1} intravenously every three days for a total of five doses. We observed no adverse effects such as weakness, bending over and weight loss during the monitoring period. Hematoxylin & eosin (H&E) staining revealed no observable lesions in major organs two weeks post the last treatment (Fig. 5). The results showed the good safety profile of PsiRNA under the repeated dosing regimen.

3. Methods and materials

Cell lines and animals

B16-F10 and LLC cell lines were purchased from the American Type Culture Collection. HEK293T and EL4 cell lines were kindly provided by Zhang's lab from Soochow University. B16-F10, EL4 and LLC cell lines were cultured in RPMI-1640 medium containing 10% FBS, 1% penicillin, and 1% streptomycin. HEK293T cell lines were cultured in DMEM containing 10% FBS, 1% penicillin and 1% streptomycin. All cell lines were cultured at 37 °C with 5% CO_2. Female C57BL/6 (6–8 weeks) were purchased from the Charles River company (Beijing, China) and maintained under the protocols approved by the Soochow University Laboratory Animal Center. All animal experiments were approved by the Animal Care and Use Committee of Soochow University and all protocols conformed to the Guide for the Care and Use of Laboratory Animals.

Preparation of conventional primary T cells

For the isolation of conventional primary T cells, single-cell suspensions were prepared from spleens of C57BL/6 mice, and incubated with Biotin-labeled anti-mouse CD3 antibody (Biolegend, San Diego, USA) at 4 °C for 20 min. After being washed with PBS, the cells were incubated with Streptavidin-labeled microbeads (Miltenyi Biotec, Germany) at 4 °C for 20 min and then subjected to the isolation of $CD3^+$ T cells according to the manufacturer's protocol (Miltenyi Biotec). Primary T cells were cultured at a density of 2×10^6 cells per mL in the RPMI-1640 medium containing 10% FBS, 1% penicillin and 1% streptomycin.

Plasmid synthesis

The sequence coding for Cbl-b was amplified from C57BL/6 mouse thymus cDNA and cloned into the pcDNA3.1(+) basic vector between the Kpnl and Xhol sites. The sequence of primers used for *cblb* cloning is: forward 5′-3′ CGGGGTA

Published on 21 February 2025. Downloaded by Soochow University China on 4/17/2026 7:33:40 AM.

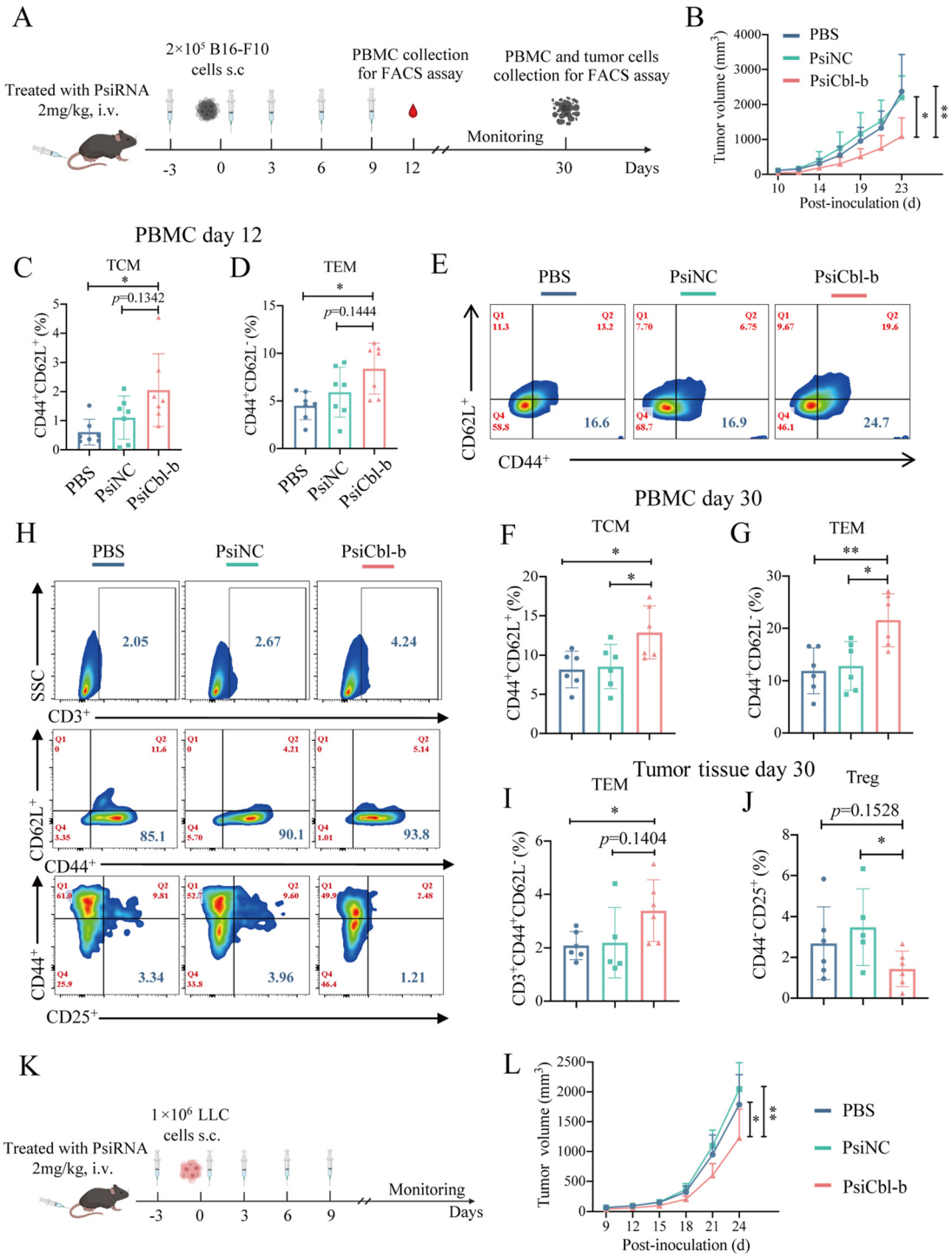

Fig. 4 PsiCbl-b significantly improves therapeutic efficacy for solid tumors. (A) Timeline for PsiRNA treatment in the murine melanoma model. C57BL/6 mice were administered with PBS, PsiNC and PsiCbl-b every three days for a total of five dosages starting on day −3. 2×10^5 B16-F10 cells were subcutaneously inoculated on the right flank on day 0. PBMCs were collected for the FACS assay three days after the last treatment. On day 30, immune cells were obtained from the tumor tissue and PBMCs were also obtained for analysis by FACS. (B) Tumor growth curve (n = 9–10). (C and D) PBMCs were collected for the FACS assay on day 12 for the quantification of (C) TCM ($CD44^+CD62L^+$) and (D) TEM ($CD44^+CD62L^-$) (n = 7). (E–G) Expression of CD44 and CD62L by T cells in collecting PBMCs on day 30, (E) representative flow cytometry plots and quantitative analysis of the percentage of (F) TCM and (G) TEM in $CD3^+$ cells (n = 6). (H–J) Tumor tissue was prepared for single-cell suspension and lymphocytes were obtained by centrifugation after treatment with the lymphocyte isolation solution. (H) Expression of $CD3^+$, $CD44^+$, $CD62^+$ and $CD25^+$ by lymphocytes in the tumor tissue and quantitative analysis of the percentage of (I) TEM and (J) Treg cells ($CD4^+CD44^-CD25^+$) (n = 5–6). (K) Timeline for PsiRNA treatment in the LLC model. C57BL/6 mice were administered with PBS, PsiNC and PsiCbl-b every three days for a total of five dosages starting on day −3. 1×10^6 LLC cells were subcutaneously inoculated on the right flank on day 0 and (L) the tumor growth curve was monitored (n = 10). P value: *$p < 0.05$; **$p < 0.01$.

This journal is © The Royal Society of Chemistry 2025

Published on 21 February 2025. Downloaded by Soochow University China on 4/17/2026 7:33:40 AM.

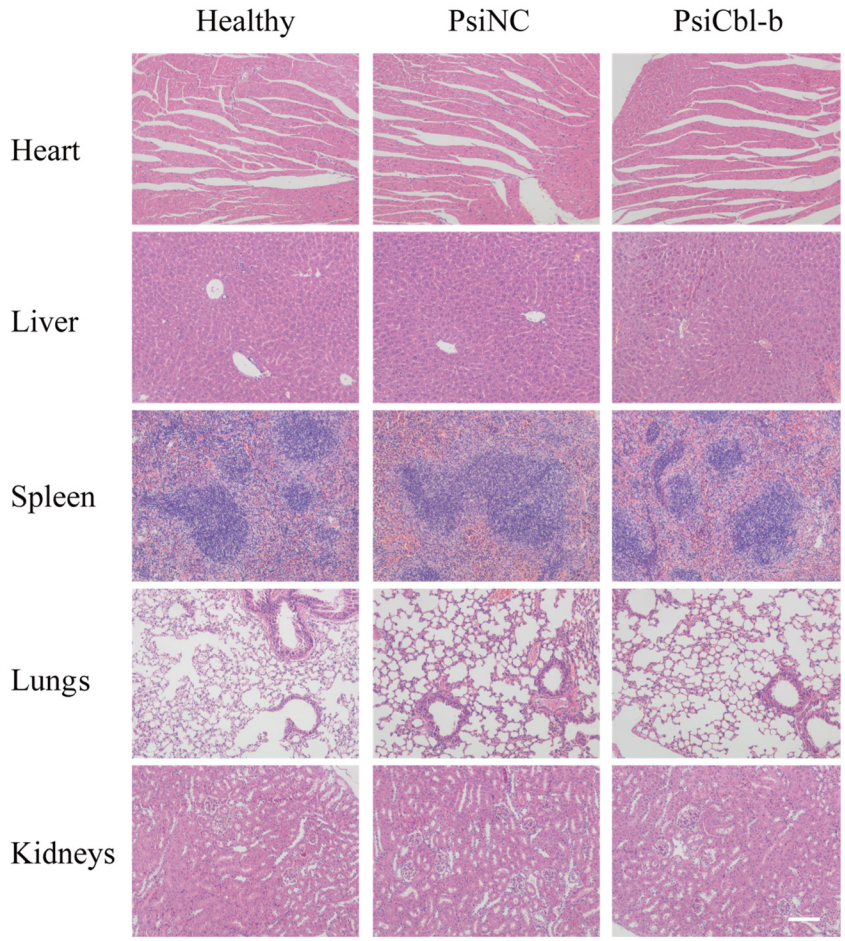

Fig. 5 Evaluation of PsiRNA toxicity *in vivo*. Representative H&E images of major organs, scale bar: 100 μm.

CCGCCACCATGGCAAATTCTATGAATGGCA, reverse 5′-3′ CCGC TCGAGCTACAGATCCTCTTCTGAGATGAGTTTTTGTTCTAGATT CAGACGTGGGGAGA.

Quantitative real-time PCR (qPCR)

Total RNA was extracted from the HEK293T cell line or sorted $CD3^+$ T using the RNAiso Plus reagent (TaKaRa, Dalian, China). First-strand complementary DNAs (cDNAs) were synthesized using oligo(dT)s and the reverse transcriptase M-MLV kit (TaKaRa, Dalian, China). qPCR was performed on a 7900H sequence detection system (Applied Biosystems, USA). Quantification of all target genes was carried out by normalizing them against the control gene β-actin. The sequences of primers used in qPCR are: Cbl-b (forward 5′-3′ TCCAGC TTAAATGGGAGGCA, reverse 5′-3′ TGGAAAAGACCTTG GCTCCT), β-actin (forward 5′-3′AACAGTCCGCCTAGAAGCAC, and reverse 5′-3′ CGTTGACATCCGTAAAGACC). Primers were synthesized by GENEWIZ (Suzhou, China).

Western blot assay

Cells were lysed in NP-40 lysis buffer (50 mM Tris, pH 7.4, 150 mM NaCl, 1% NP-40, sodium pyrophosphate, β-glycerophosphate, sodium orthovanadate, sodium fluoride, EDTA, and leupeptin) containing 1 mM PMSF (phenylmethane-sulfonyl fluoride) and immunoblotting was conducted following standard procedures. The following antibodies were used in our study: anti-Cbl-b (D3C12) (#9498) was purchased from Cell Signaling Technology (Danvers, MA, USA); anti-Flag and anti-β-actin antibodies were purchased from Affinity Biosciences (USA); HRP-conjugated goat anti-rabbit antibodies were used as secondary antibodies.

Synthesis and characterization of PsiRNA

Poly(ethylene glycol)-*b*-poly(trimethylene carbonate-*co*-dithiolane trimethylene carbonate)-polyethyleneimine (abbreviated as PEG-P(TMC-DTC)-PEI) was synthesized as reported previously.[26] Briefly, the preparation of block copolymers was conducted by ring opening polymerization of TMC and DTC through macromolecular initiators. To prepare PsiRNA with a theoretical loading of 10 wt%, 100 μL of PEG-P(TMC-DTC)-PEI (40 mg mL^{-1}) in *N*,*N*-dimethylformamide (DMF) was added to phosphate buffer (PB, pH 6.0, 2 mM, 900 μL) containing siRNA (2 mg mL^{-1}, 400 μg) under stirring at 300 rpm. After stirring at RT for 10 min, the dispersion was dialyzed against PBS (pH

Published on 21 February 2025. Downloaded by Soochow University China on 4/17/2026 7:33:40 AM.

7.4, 10 mM) for 6 h (MWCO 1000 kDa) to remove DMF and unencapsulated siRNA. Size distribution was measured by dynamic light scattering (DLS) and transmission electron microscopy (TEM). The amount of siRNA loaded was determined using a NanoDrop spectrophotometer. The drug loading content (DLC) and drug loading efficiency (DLE) were calculated based on the following formulas:

$$\mathrm{DLC\,(wt\%)} = \frac{\text{weight of loaded drug}}{\text{total weight of loaded drug and polymers}} \times 100\%$$

$$\mathrm{DLE\,(\%)} = \frac{\text{weight of loaded drug}}{\text{weight of drug in feed}} \times 100\%$$

Transfection of HEK293T and primary T cells *in vitro*

For co-transfection with Cbl-b plasmid and siRNA in HEK293T cells, HEK293T cells were seeded in 24 well plates with 2×10^5 per well for overnight culture. Then the medium was replaced with 0.5 mL of serum-free DMEM, and the co-transfection progress was monitored according to the manufacturer's protocol of Lipofectamine™ 2000 (Invitrogen, USA). For example, for the amount used per well, 2.0 μL of the Lipofectamine™ reagent was diluted in 25 μL of the serum-free DMEM medium. Then 0.5 μg of Cbl-b plasmid and 20 pmol siRNA were diluted in 25 μL of serum-free DMEM medium, and the diluted plasmid and siRNA were added to the diluted Lipofectamine™ reagent at a 1 : 1 ratio. After incubating for 5 min, the lipid complex was added to the cells for 4 h of transfection, and then the medium was replaced with a normal DMEM medium and cultured for 72 h.

For transfection with PsiRNA in HEK293T cells, the steps for overexpression of Cbl-b in HEK293T cells were the same as above. Then PsiRNA (siRNA Conc. 50 nM, 100 nM and 200 nM; siNC Conc. 200 nM) was added to the cells and cultured for 72 h.

Primary T cells (2×10^6 cells and 0.5 mL medium per well) were incubated in 24 well plates without the step of overexpressing Cbl-b, and PsiRNA (siRNA Conc. 200 nM) was directly added to the cells and cultured for 72 h. Fresh medium was supplemented with 0.5 mL every 24 h.

Safety evaluation of PsiRNA

For the safety profile study, *in vitro* primary T cells were inoculated in 96 well plates with 20,000 cells per well, PsiRNA was added in different concentrations (NPs conc. 5, 25, 50, 100, and 200 μg mL^{-1}) for co-culturing for 24 h. Cell viability was analyzed *via* the CCK-8 cytotoxicity assay (Meilunbio, Dalian, China) following the manufacturer's instruction (n = 5). The *in vivo* H&E staining was conducted using a Servicebio® kit according to manufacturer's instructions.

$$\mathrm{Cell\,viability\,(\%)} = \frac{\mathrm{OD_{experiment}} - \mathrm{OD_{blank}}}{\mathrm{OD_{control}} - \mathrm{OD_{blank}}} \times 100\%$$

Endosomal escape of PsiRNA^{Cy5}

Primary T cells were plated in a glass-bottomed dish (1×10^7 per well) and cultured with PsiRNA^{Cy5} (200 mM). After being co-cultured for 4 h, the cells were incubated with 50 nM Lysotracker red (Beyotime, Shanghai, China) at 37 °C with 5% CO_2 for 30 min. Then T cells were washed with cold PBS and further cultured with a 2 μM DiO cell membrane fluorescent probe (Biosharp, Anhui, China) at 37 °C for 20 min. After washing with PBS three times, T cells were fixed with 4% paraformaldehyde solution for 20 min and then resuspended in antifade mounting medium (MCE, Shanghai, China) before CLSM observation.

Evaluation of activation of primary T cells

Primary T cells were cultured in 24-well plates (2×10^6 per well). After 4 h, T cells were incubated with PBS, PsiNC, and PsiCbl-b (weight ratio of NPs : siRNA = 10 : 1, siRNA 200 nM, n = 3) at 37 °C under a 5% CO_2 atmosphere. The medium supernatant was collected at 48 h to detect the secreted IFN-γ and TNF-α by the ELISA assay. After 72 h, the cells were centrifuged and washed with FACS buffer (1% FBS in PBS), incubated with anti-CD16/32 at RT, and then stained with CD3-FITC and CD25-PE/Cy7, for 20 min at RT. The cells were then washed twice using FACS buffer and detected using a flow cytometer.

Adoptive transfer mouse model

Primary T cells were treated with PBS, empty vehicle NPs, PsiNC and PsiCbl-b for 72 h (siRNA Conc. 200 nM, NPs Conc. 26 μg mL^{-1}). C57BL/6 mice were inoculated with 2×10^5 EL4 cells subcutaneously on the right flank and injected with 2×10^6 treated T cells intravenously on day 0. Tumor volume was calculated using the following equation: tumor volume = length × width^2 × 0.5.

Biodistribution of PsiRNA *in vivo*

Mice were intravenously injected with free siRNA^{Cy5} and PsiRNA^{Cy5} respectively (siRNA^{Cy5} 1 mg kg^{-1} per mouse). After 20 hours, the mice were euthanatized and their organs were harvested to analyze the biodistribution of PsiRNA *via* IVIS imaging.

Transfection of T cells *in vivo*

Mice were intravenously injected with PBS, PsiNC and PsiCbl-b respectively (siRNA 2 mg kg^{-1} per mouse). After 72 hours, $CD3^+$ T cells were sorted from the splenocytes of mice to extract RNA for qPCR analysis.

Evaluation of anti-tumor efficacy of PsiRNA

For the LLC non-small cell lung cancer model, mice were treated every three days from day −3 for a total of five doses with PBS, PsiNC and PsiCbl-b respectively (siRNA, 2 mg kg^{-1}, I.V.). 1×10^6 LLC cells were inoculated subcutaneously on the right flank of mice on day 0, and tumor growth was monitored until 24 days.

For the B16-F10 melanoma model, mice were treated every three days from day −3 for a total of five doses with PBS, PsiNC and PsiCbl-b respectively (siRNA, 2 mg kg^{-1}, I.V.). 2×10^5 B16-F10 cells were inoculated subcutaneously on the right flank of mice on day 0, and the tumor volume was monitored for

 This journal is © The Royal Society of Chemistry 2025

Published on 21 February 2025. Downloaded by Soochow University China on 4/17/2026 7:33:40 AM.

23 days. PBMCs were collected on day 12 and resuspended in ACK lysis buffer to remove red blood cells. The cells were then centrifuged and incubated with anti-CD16/32 at RT and stained with CD3-FITC, CD44-PE and CD62L-APC/Cy7 for 30 min. The cells were then washed twice using FACS buffer and analyzed using a flow cytometer. The mice were sacrificed on day 30; the tumor tissue was prepared for single-cell suspension and lymphocytes were obtained by centrifugation after treatment with the lymphocyte isolation solution. Lymphocytes were incubated with anti-CD16/32 at RT and stained with CD3-FITC, CD44-PE, and CD62L-APC to analyze the TEM and stained with CD4-APC, CD44-FITC and CD25-PE to analyze the Treg cells. PBMCs were stained as well in the manner we previously stained them on day 12.

Statistical analysis

All data are presented as mean ± standard deviation (SD). To assess the statistical significance of different treatment groups, we used one-way ANOVA comparisons or unpaired two-tailed Student's *t* tests in two different treatments for comparison using GraphPad Prism (version 8). *, $p < 0.05$; **$p < 0.01$; ***$p < 0.001$ and ****$p < 0.0001$, and ns indicates not significant. p values less than 0.05 were considered statistically significant. The data represent three independent experiments unless indicated.

4. Conclusion

Moldulation of T cells *in vivo* is critical for immunotherapy, yet directly stimulating T cells poses significant challenges. We present a polymersome delivery platform that directly activates T cells *in vivo*. The polymersomes successfully transfected T cells both *in vivo* and *in vitro* to reduce *cblb* gene expression and enhance T cell function for a robust anti-tumor response. This strategy provides new opportunities for *in vivo* T cell modulation and has great potential as a safe and versatile delivery platform for clinical translation. In future work, we would take a closer look at the T cell targeting efficiency and the anti-tumor effect of NK cells. In addition, *in vivo* T cell modulation coupled with immune checkpoint blockade therapy will be explored. More importantly, we expect that prolonging the circulation of siRNA through chemical modification and improving the efficiency of T-cell targeting would further enhance the clinical application prospects of this strategy.

Author contributions

Guanhong Cui: writing – original draft, validation, project administration, methodology, investigation, and conceptualization. Yu Shao: validation, methodology, investigation, and formal analysis. Junyao Wang: methodology and formal analysis. Congcong Xu: writing – review & editing, formal analysis, and data curation. Jinping Zhang: methodology, investigation, conceptualization, supervision, and resources. Zhiyuan Zhong: writing – review & editing, supervision, funding acquisition, and conceptualization.

Data availability

Data for this article are available at BaiduNetdisc at **https://pan.baidu.com/s/1oszqHnA4qA00kGw62CcJjw**, password: 94hd.

Conflicts of interest

The authors declare that they have no known competing financial interests or personal relationships that could have appeared to influence the work reported in this paper.

Acknowledgements

This work was supported by the National Key R&D Program of China (2021YFB3800900) and the National Natural Science Foundation of China (52233007, 82071765). Congcong Xu is sponsored by the Shanghai Pujiang Talent Program (22PJ1423100). All the animal experiments were approved by the Animal Care and Use Committee of Soochow University (Suzhou, China), and all protocols of animal studies conformed to the Guide for the Care and Use of Laboratory Animals (approval no. SYXK 2021-0065).

References

1 S. P. Kubli, T. Berger, D. V. Araujo, L. L. Siu and T. W. Mak, *Nat. Rev. Drug Discovery*, 2021, **20**, 899–919.
2 D. J. Baker, Z. Arany, J. A. Baur, J. A. Epstein and C. H. June, *Nature*, 2023, **619**, 707–715.
3 M. J. Lin, J. Svensson-Arvelund, G. S. Lubitz, A. Marabelle, I. Melero, B. D. Brown and J. D. Brody, *Nat. Cancer*, 2022, **3**, 911–926.
4 D. S. Thommen and T. N. Schumacher, *Cancer Cell*, 2018, **33**, 547–562.
5 A. Schietinger and P. D. Greenberg, *Trends Immunol.*, 2014, **35**, 51–60.
6 Q. Wang, Y. Qin and B. Li, *Cancer Lett.*, 2023, **559**, 216043.
7 G. Wei, H. Zhang, H. Zhao, J. Wang, N. Wu, L. Li, J. Wu and D. Zhang, *Cancer Lett.*, 2021, **511**, 68–76.
8 R. W. Jenkins, D. A. Barbie and K. T. Flaherty, *Br. J. Cancer*, 2018, **118**, 9–16.
9 M. S. Carlino, J. Larkin and G. V. Long, *Lancet*, 2021, **398**, 1002–1014.
10 A. S. D. Galy, S. Menegatti, J. Fuentealba, F. Lucibello, L. Perrin, J. Helft, A. Darbois, M. Saitakis, J. Tosello, D. Rookhuizen, M. Deloger, P. Gestraud, G. Socie, S. Amigorena, O. Lantz and L. Menger, *Sci. Immunol.*, 2021, **6**, eabe8219.
11 J. Wei, L. Long, W. Zheng, Y. Dhungana, S. A. Lim, C. Guy, Y. Wang, Y.-D. Wang, C. Qian, B. Xu, A. Kc, J. Saravia,

Published on 21 February 2025. Downloaded by Soochow University China on 4/17/2026 7:33:40 AM.

H. Huang, J. Yu, J. G. Doench, T. L. Geiger and H. Chi, *Nature*, 2019, **576**, 471–476.
12 K. Bachmaier, C. Krawczyk, I. Kozieradzki, Y.-Y. Kong, T. Sasaki, A. Oliveira-dos-Santos, S. Mariathasan, D. Bouchard, A. Wakeham, A. Itie, J. Le, P. S. Ohashi, I. Sarosi, H. Nishina, S. Lipkowitz and J. M. Penninger, *Nature*, 2000, **403**, 211–216.
13 Y. P. J. Chiang, H. K. Kole, K. Brown, M. Naramura, S. Fukuhara, R. J. Hu, I. K. Jang, J. S. Gutkind, E. Shevach and H. Gu, *Nature*, 2000, **403**, 216–220.
14 M. Paolino, C. B. F. Thien, T. Gruber, R. Hinterleitner, G. Baier, W. Y. Langdon and J. M. Penninger, *J. Immunol.*, 2011, **186**, 2138–2147.
15 G. P. Collins, W. Townsend, A. Abdulgawad, S. Namburi, A. Williams, A. F. P. DosReis, M. G. Krebs, J. Evans, S. P. Blagden, R. Plummer, D. Hochhauser, A. Sharp, G. Cole, S. Rogers, D. Chan, S. Whelan and D. El-Sharkawi, *Blood*, 2023, **142**, 3093–3095.
16 S. W. Kimani, S. Perveen, M. Szewezyk, H. Zeng, A. Dong, F. Li, P. Ghiabi, Y. Li, I. Chau, C. H. Arrowsmith, D. Barsyte-Lovejoy, V. Santhakumar, M. Vedadi and L. Halabelian, *Commun. Biol.*, 2023, **6**, 1272.
17 P. Triozzi, M. Kooshki, A. Alistar, R. Bitting, A. Neal, G. Lametschwandtner and H. Loibner, *J. Immunother. Cancer*, 2015, **3**, P175.
18 R. Gugenberger, A. Dohnal, A. Tanzmann, B. Pribitzer, F. Batrina, S. Bunka, S. Spagl, M. Branka, S. Bischof, K. Thell, M. Kuttke, M. Urban, H. Muehleisen, B. Peball, M. Raderer, G. Prager and N. Worel, *J. Immunother. Cancer*, 2022, **10**, A755.
19 J. Kumar, R. Kumar, A. Kumar Singh, E. L. Tsakem, M. Kathania, M. J. Riese, A. L. Theiss, M. L. Davila and K. Venuprasad, *J. Immunother. Cancer*, 2021, **9**, e001688.
20 R. Hinterleitner, T. Gruber, C. Pfeifhofer-Obermair, C. Lutz-Nicoladoni, A. Tzankov, M. Schuster, J. M. Penninger, H. Loibner, G. Lametschwandtner, D. Wolf and G. Baier, *PLoS One*, 2012, **7**, e44295.
21 H. Loibner, G. Lametschwandtner, K. Westritschnig, O. Mutschlechner, A. Dohnal, M. O. Salzberg and P. L. Triozzi, *J. Clin. Oncol.*, 2018, **36**, 3055.
22 R. C. Larson and M. V. Maus, *Nat. Rev. Cancer*, 2021, **21**, 145–161.
23 S. Ramishetti and D. Peer, *Adv. Drug Delivery Rev.*, 2019, **141**, 55–66.
24 A. R. K. Kumar, Y. Shou, B. Chan and K. L. A. Tay, *Adv. Mater.*, 2021, **33**, 2007421.
25 D. Berdecka, S. C. De Smedt, W. H. De Vos and K. Braeckmans, *Adv. Drug Delivery Rev.*, 2024, **208**, 115215.
26 Z. Wang, S. Zhao, J. Shi, F. Meng, J. Yuan and Z. Zhong, *Acta Biomater.*, 2022, **138**, 443–452.
27 R. Huang, H. Du, L. Cheng, P. Zhang, F. Meng and Z. Zhong, *Acta Biomater.*, 2023, **168**, 529–539.
28 Y. Wei, Y. Sun, J. Wei, X. Qiu, F. Meng, G. Storm and Z. Zhong, *J. Controlled Release*, 2021, **337**, 521–529.
29 J. Casper, S. H. Schenk, E. Parhizkar, P. Detampel, A. Dehshahri and J. Huwyler, *J. Controlled Release*, 2023, **362**, 667–691.
30 F. Hao, Y. Li, J. Zhu, J. Sun, B. Marshall, R. J. Lee, L. Teng, Z. Yang and J. Xie, *Curr. Med. Chem.*, 2019, **26**, 2264–2284.
31 K. M. Brown, J. K. Nair, M. M. Janas, Y. I. Anglero-Rodriguez, L. T. H. Dang, H. Y. Peng, C. S. Theile, E. Castellanos-Rizaldos, C. Brown, D. Foster, J. Kurz, J. Allen, R. Maganti, J. Li, S. Matsuda, M. Stricos, T. Chickering, M. C. Jung, K. Wassarman, J. Rollins, L. Woods, A. Kelin, D. C. Guenther, M. W. Mobley, J. Petrulis, R. McDougall, T. Racie, J. Bombardier, D. A. Cha, S. Agarwal, L. Johnson, Y. F. Jiang, S. Lentini, J. Gilbert, T. Nguyen, S. Chigas, S. LeBlanc, U. Poreci, A. Kasper, A. B. Rogers, S. H. Chong, W. Davis, J. E. Sutherland, A. Castoreno, S. Milstein, M. K. Schlegel, I. Zlatev, K. Charisse, M. Keating, M. Manoharan, K. Fitzgerald, J. T. Wu, M. A. Maier and V. Jadhav, *Nat. Biotechnol.*, 2022, **40**, 1500–1508.
32 B. B. Mendes, J. Conniot, A. Avital, D. Yao, X. Jiang, X. Zhou, N. Sharf-Pauker, Y. Xiao, O. Adir, H. Liang, J. Shi, A. Schroeder and J. Conde, *Nat. Rev. Methods Primers*, 2022, **2**, 24.
33 T. R. Abreu, N. A. Fonseca, N. Goncalves and J. N. Moreira, *J. Controlled Release*, 2020, **319**, 246–261.
34 J. Liu, M. Fu, M. Wang, D. Wan, Y. Wei and X. Wei, *J. Hematol. Oncol.*, 2022, **15**, 28.
35 M. S. Jeon, A. Atfield, K. Venuprasad, C. Krawczyk, R. Sarao, C. Elly, C. Yang, S. Arya, K. Bachmaier, L. Su, D. Bouchard, R. Jones, M. Gronski, P. Ohashi, T. Wada, D. Bloom, C. G. Fathman, Y. C. Liu and J. M. Penninger, *Immunity*, 2004, **21**, 167–177.
36 C. Lutz-Nicoladoni, D. Wolf and S. Sopper, *Front. Oncol.*, 2015, **5**, 58.

 This journal is © The Royal Society of Chemistry 2025